Model of UAV and Downwash for Multi-UAV Path Planning

Chih-Chun Chen* and Hugh H.-T. Liu †
Institute for Aerospace Studies, University of Toronto, 4925 Dufferin St, North York, Ontario, Canada, M3H 5T6

This paper develops a method to model the air flow downwash effect generated by the quadrotor unmanned aerial vehicle (UAV) and its effect on the neighboring UAVs. The downwash model derives the resultant downwash force and torque and takes the UAV attitude into the account. Each UAV is shaped by a virtual structure for collision-free path planning. The shape is modified from a standard spherical body to a proposed cylinder to better minimize downwash impact. A flock-based path planning algorithm and an optimal reciprocal collision avoidance (ORCA) algorithm are implemented and investigated in this study to analyze the downwash effect and the performance of the proposed cylindrical shape UAV model. The downwash model simulation shows how the UAV can be affected when it counters the downwash air flow. A flock-based algorithm and an ORCA algorithm along with the spherical and cylindrical shape UAV models are simulated to demonstrate the cylindrical model can improve path planning performance.

Nomenclature

f_{dw}	=	downwash force, N
a_{dw}	=	UAV deceleration due to downwash effect, (m/s^2)
r_{uav}	=	radius of the real UAV, m
r_α	=	the interaction radius of the UAV model, m
h_α	=	the interaction height of the UAV model, m
V_{max}	=	maximum allowable velocity, m/s
a_{max}	=	maximum allowable acceleration, m/s^2
$\mathbf{f_i^R}$	=	repulsive force on ith UAV from flock-based algorithm, N (m/s^2)
$\mathbf{f_i^\gamma}$	=	navigational feedback on ith UAV from flock-based algorithm, N (m/s^2)

I. Introduction

MULTIPLE unmanned aerial vehicles (multi-UAV) path planning has been a popular research topic for decades, and it can be utilized in various applications, such as surveillance [1], formation flight [2], and even entertainment [3]. One of the key requirements of the multi-UAV path planning problem is that all UAVs successfully travel from their initial locations to assigned targets without any collision.

Many path planning researches address the challenges of existing algorithms in different aspects, such as the navigation through obstacle rich environments [4], the computational efficiency [5], and the solution optimality [6]. However, very little research addresses the downwash effect which presents a real challenge in close encounters among multi-rotor UAVs. The downwash is the induced force generated beneath the UAV rotors due to the large volume of air flow to gain the upward lift. For example, the downwash effect can let an UAV lose stability and collide with neighboring UAVs, or crash to the ground. In fact, the downwash force is an existing factor that becomes an issue that cannot be ignored in the real multi-UAV experiment, especially in a three-dimensional (3D) dense environment.

On one hand, a strong downwash air flow can cause the UAV underneath to lose stability, change attitude, and drop altitude. On the other hand, a weak downwash air flow can have a minor influence on an UAV. The downwash air flow intensity depends on the rotor spinning speed and the distance travelled since the air flow velocity is proportional to the rotor spinning rate and air diffuses while travelling. If the downwash effect intensity is accessible, the UAV's behaviour due to downwash would be predictable. Some literature presents methods to obtain the downwash air flow intensity.

*MASc student, Institute for Aerospace Studies, University of Toronto, 4925 Dufferin St, North York, Ontario, Canada, M3H 5T6
†Professor, Institute for Aerospace Studies, University of Toronto, 4925 Dufferin St, North York, Ontario, Canada, M3H 5T6, AIAA Associate Fellow

Yeo et al. [7] implemented a pressure-probe flow measurement system on the quadrotors to sense the downwash air flow velocity. Wu et al. [8] designed a downwash air flow detection system from the full-bridge strain effect principle. However, both of these methods required the UAV to install an additional instrument to collect downwash effect data and to suffer from the downwash effect before getting the downwash air flow data. UAVs would not be able to react fast enough to avoid the downwash air flow when they collect the data and predict the air flow is harmful.

Once the downwash air flow intensity is available, the influence on any UAV that counters the air flow shall be determinable. To address the downwash problem from the path planning point of view, an UAV can decide to avoid this unsafe vertical region the way it avoids a collision. Hönig et al. [9] [10] modelled the UAVs as axis-aligned ellipsoids, and Ferrera et al. [11] modelled the UAVs as cylinders. Both ellipsoid and cylindrical shapes allow the UAVs to enlarge their vertical distance since the path planning algorithm would prevent their modelled shape being collided. Figure 1 demonstrates the usual spherical UAV field model in light blue, the cylindrical model is purple, and the downwash airflow is yellow.

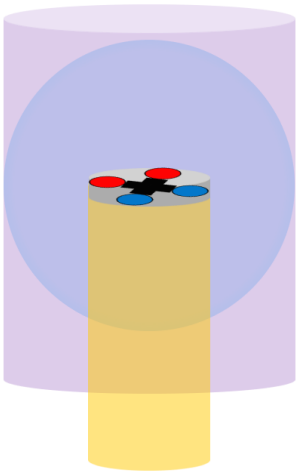

Fig. 1 UAV models

However, extra space to avoid collisions would lead to reducing in path planning algorithm performance. There is a trade-off between downwash avoidance and performance. When considering the cylindrical shape, the size of the volume and the height matter. The cylinder height needs to be sufficiently tall, that UAVs will not be vertically close to each other and the downwash force exerted on the underneath UAV is insignificant since the downwash force decreases as the vertical distance increase. Nevertheless, the cylinder with a large height number may affect the performance negatively. For example, the transition time for all UAVs to travel to the desired location increases due to the increase of the UAV's volume. The extra volume also means that it requires an extra area for two UAVs to go around (avoid) each other. To the best of the authors' knowledge, none of the existing works has specified a rule to decide the geometric parameters of the UAV's field, or studied in detail the influence of those geometric properties on the multi-UAV path planning.

In this paper, a downwash model is developed and it can predict the downwash effect on an UAV without any extra instrument mounted on the UAV. The downwash model will give the relationship between downwash force and the vertical distance. The pose and position of an UAV influenced by the downwash effect will be able to be determined from the downwash model. A flock-based path planning algorithm [12] and an optimal reciprocal collision avoidance (ORCA) algorithm [13] are adopted to test for the downwash model and customized to account for the cylindrical UAV model. The performances of different algorithms and different models under the effective downwash effect are compared and analyzed.

II. Downwash Model

The downwash effect can be severe when there are multi-UAV flying in a 3D dense environment. To consider the downwash force into the multi-UAV path planning algorithm, one needs to know how significant the downwash effect can influence an UAV that is a distance away.

This section derives a downwash model used for predicting the downwash effect on the quadrotor UAVs without the aid from any of the additional sensors. The derivation utilized the UAV acceleration to obtain the downwash force and acceleration that is a vertical distance away from the UAV that produces the downwash air flow. The derivation begins with the general equations of motion of quadrotors to obtain the UAV thrust from acceleration. Next, the momentum theory utilizes the UAV thrust to obtain the air flow velocity induced by a rotor. Thirdly, the jet flow concept is applied to obtain the relationship between distance and air flow velocity. Then, the air flow velocity is converted to the downwash force. This section continues by including the UAV attitude and torque into the downwash model. The quadrotor UAVs are assumed homogeneous, meaning that all UAVs have the same weight and size. The UAVs are also assumed to have circular shapes from the top view, east-north-up (ENU) inertial and body frames, and zero yaw angles all the time.

A. Downwash Force Model

The downwash force is caused by a large volume of air flow to produce lift, which is directly related to the thrust of the UAV. The magnitude of the commanded thrust depends on the desired acceleration assume a suitable controller algorithm is available. The acceleration can be obtained from either the inertial measurement unit (IMU) sensors or the command from the path planning algorithm. The relationship between the thrust and the acceleration can be obtained from the quadrotor UAV equation of motion. The equation of motion of an UAV can be expressed as follows,

$$m\ddot{\mathbf{x}}_I = \mathbf{R_{IB}} \begin{bmatrix} 0 \\ 0 \\ T \end{bmatrix} + \begin{bmatrix} 0 \\ 0 \\ -mg \end{bmatrix} \tag{1}$$

where m is the mass of the quadrotor, $\mathbf{x} = [x,\ y,\ z]^T$ is the UAV position in the inertial frame, $m\ddot{\mathbf{x}}_I$ is the inertial force, $\mathbf{R_{IB}}$ is the rotation matrix from the body frame to the inertial frame, T is the thrust force along the z-direction of its body frame, and $g = 9.81 m/s^2$ is the acceleration due to gravity. With the acceleration input, the thrust force is determinable by reorganizing Equation 1 and is shown as follows,

$$T = m\mathbf{1_3}^T \mathbf{R_{BI}} \begin{bmatrix} \ddot{x} \\ \ddot{y} \\ \ddot{z} + g \end{bmatrix} \tag{2}$$

where $\mathbf{1_3} = [0, 0, 1]^T$. Assume the thrust force is equally generated between four rotors, the thrust generated by one rotor is $T_r = T/4$.

$$T_r = \frac{T}{4} = \frac{m}{4}\mathbf{1_3}^T \mathbf{R_{BI}} \begin{bmatrix} \ddot{x} \\ \ddot{y} \\ \ddot{z} + g \end{bmatrix} \tag{3}$$

The thrust force is produced by the air flow generated from the spin of the rotor. The faster the rotor spins, the faster the air flow velocity below the rotor, and the larger the thrust. Based on the momentum (disk actuator) theory [**?**], the relationship between the thrust (T_r) and the induced velocity (v_i) with zero free stream velocity assumption is as follows,

$$v_i = \sqrt{\frac{2T_r}{\rho_{air} A_{rotor}}} \tag{4}$$

where ρ_{air} is the air density and A_{rotor} is the area swept out by the rotor. The direction of the resultant air flow velocity v_i is the same as the thrust force T_r, which is along the negative direction of the UAV body frame z-axis.

The air flow spread out and slow down over distance. The UAV that is below and vertically further away from the UAV that produces the downwash force will suffer less from the downwash effect. Therefore, it is necessary to obtain the relationship between the air flow velocity and the distance. The jet flow concept [14] gives the relationship between the air flow velocity and the distance, so it is adopted in the downwash model derivation. Assume that the air flow velocity is uniform and maximized over the horizontal plane, the air flow velocity with respect to the vertical distance (z) is denoted as $v(z)$. Figure 2 shows the aforementioned steps.

$$v(z) = \frac{10 v_i}{z}\sqrt{\frac{A_{rotor}}{2\pi}} = \frac{10}{z}\sqrt{\frac{T_r}{\pi \rho_{air}}} \tag{5}$$

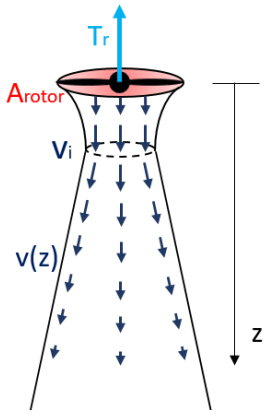

Fig. 2 Air flow underneath a rotor

When the air flow hits a surface, it exerts a force. Therefore, for an UAV that is a distance away from the upper UAV, the downwash force that it got exerted on can be calculated by converting the air flow velocity to force. Let $(x_{top}, y_{top}, z_{top})$ and $(x_{bot}, y_{bot}, z_{bot})$ be the coordination of the top and bottom UAV, respectively. It is assumed that the diffused air flow is negligible, so the bottom UAV will suffer from the downwash force when the top UAV overlaps it over the z-axis. This overlap can also be expressed mathematically as $(x_{top} - x_{bot})^2 + (y_{top} - y_{bot})^2 \leq r_{uav}$, where r_{uav} is the radius of the UAV. It is assumed that the mixed air flow from all four rotors does not influence the maximum air flow velocity, and the air flow velocity is uniform over xy plane with given z. It is also assumed that the downwash air flow does not influence UAV thrust and the propeller. The downwash force and acceleration exerted on the bottom UAV with a given vertical distance difference $(z = z_{top} - z_{bot})$ are as follows,

$$f_{dw}(z) = -\frac{1}{2}\rho_{air} c_d A_{exert} v^2(z) = -\frac{50 c_d A_{exert}}{\pi} \frac{T_r}{z^2} \tag{6}$$

$$a_{dw}(z) = \frac{f_{dw}(z)}{m} = -\frac{25 c_d A_{exert}}{2\pi z^2} \mathbf{1_3}^T \mathbf{R_{BI}} \begin{bmatrix} \ddot{x} \\ \ddot{y} \\ \ddot{z} + g \end{bmatrix} \tag{7}$$

where A_{exert} is the UAV surface area that the air flow hits on. c_d is the drag coefficient and is 1.28 in the worst case where the air flow hits the disc-shape UAV perpendicularly. Both the downwash force and the acceleration expressed in Equations 6 and 7 are scalars. The negative signs represent that the downwash force direction is pointing downward along the negative z-axis of the UAV body frame, which is equivalent to the opposite direction of the norm of the UAV surface. The bottom UAV z meters vertically away from the top UAV is being pushed downward by an acceleration of $a_{dw}(z)$ from the downwash effect.

B. Tilted Downwash Effect

The downwash air flow direction is along the negative direction of the UAV body frame z-axis. Therefore, as the UAV rolls and pitches, the downwash airflow changes its direction. The lower UAV that suffers from the downwash would no longer suffer from a vertical force only, but also horizontal force. Moreover, there exists an induced torque if the center of the air flow does not hit the UAV's center of mass. This section derives the downwash airflow direction and its impact on the lower UAV. The derivation of the induced torque by downwash air flow is also presented in this section.

As the downwash air flow direction changes, the lower UAV that may suffer from downwash will be redefined. For some rare cases, the lower UAV that is right below the top UAV may not suffer from downwash, and the lower UAV that is a horizontal distance away from the top UAV may also suffer from downwash. It all depends on the attitude of the top UAV.

To determine whether an UAV would suffer from the downwash force, it shall discover whether it will be hit by any of the downwash air flow. It will suffer from the downwash force if it is below the top UAV from the top UAV's

body frame perspective. Therefore, the two UAV's position relative to the top UAV's body frame is crucial to the determination. The position relationship between two UAVs, UAV1 and UAV2, can be described as follows,

$$\mathbf{p_2} = \mathbf{p_1} + \mathbf{R_{IB_1}}\mathbf{d_{12}} \tag{8}$$

where $\mathbf{p_1}, \mathbf{p_2} \in \mathbb{R}^3$ are the position of the two UAVs' center of mass in the inertial frame, R_{IB_1} is the rotation matrix from the UAV1 body frame to the inertial frame, and $\mathbf{d_{12}} \in \mathbb{R}^3$ is the distance from UAV1 to UAV2 in the UAV1 body frame. Reorganize Equation 8, the distance between the two UAVs in UAV1 body frame is,

$$\mathbf{d_{12}} = [d_{12_x},\, d_{12_y},\, d_{12_z}]^T = \mathbf{R_{B_1I}}(\mathbf{p_2} - \mathbf{p_1}) \tag{9}$$

On one hand, if $d_{12_z} > 0$, UAV1 has a lower altitude than the UAV2 from the UAV1 perspective because the initial frame is an ENU frame. On the other hand, if $d_{12_z} < 0$, UAV1 has a higher altitude than the UAV2, and if $d_{12_x}^2 + d_{12_y}^2 \leq (2\, r_{uav})^2$, the downwash air flow produced by UAV1 can exert on UAV2. UAV2 will suffer from the downwash effect, and the z parameter indicated in Equation 6 and 7 in the downwash equation is replaced by d_{12_z}.

$$a_{dw}(z) = a_{dw}(d_{12_z}) = -\frac{25 c_d A_{exert}}{2\pi d_{12_z}^2} \mathbf{1_3}^T \mathbf{R_{BI}} \begin{bmatrix} \ddot{x}_1 \\ \ddot{y}_1 \\ \ddot{z}_1 + g \end{bmatrix} \tag{10}$$

The downwash air flow direction is along the negative z-axis of UAV1. Therefore, from UAV1's point of view, UAV2 is suffering from the following downwash acceleration,

$$\mathbf{a_{dw_{B_1}}}(d_{12_z}) = \begin{bmatrix} 0 \\ 0 \\ a_{dw}(d_{12_z}) \end{bmatrix} \tag{11}$$

From the initial frame point of view, the downwash effect is letting UAV2 decelerating in the direction and magnitude of,

$$\mathbf{a_{dw_I}}(d_{12_z}) = \mathbf{R_{IB_1}}\mathbf{a_{dw_{B_1}}}(d_{12_z}) \tag{12}$$

$$= a_{dw}(d_{12_z})\mathbf{R_{IB_1}}\mathbf{1_3} \tag{13}$$

In the previous section, only downwash force/acceleration is considered, this is correct if the air flow hits the center of mass of an UAV. However, this is usually not the case. For example, the downwash air flow only hits the edge of the bottom UAV, then the UAV does not only receive the downwash force but also the torque, resulting in extra roll or pitch. This section derives the amount of torque exerted on the UAV due to the downwash air flow.

Consider the fundamental torque equation,

$$\tau = F_\perp L = I\alpha \tag{14}$$

where τ is the torque, $F_\perp$ is the force in the direction perpendicular to the surface, L is the distance from the center to the location where force is applied, I is the moment of inertia, and α is the angular acceleration.

Let UAV1 be the top UAV and UAV2 be the bottom UAV, the downwash force exerted on UAV2 in the inertial frame is $m\mathbf{a_{dw_I}}(d_{12_z})$, and this force expressed in the UAV2 body frame is,

$$\mathbf{F_{dw,B_2}} = m\mathbf{R_{B_2I}}\mathbf{a_{dw_I}}(d_{12_z}) \tag{15}$$

The third entry of the $\mathbf{F_{dw,B_2}}$ vector, is the component where the downwash force is perpendicular to the surface area of the UAV2.

$$F_\perp = m\mathbf{1_3^T}\mathbf{R_{B_2I}}\mathbf{a_{dw_I}}(\mathbf{d_{12_z}}) \tag{16}$$

The distance from the force exerted point to the center of the UAV is expressed as $L = (d_{12_x}^2 + d_{12_y}^2)^{0.5}/2$. For a thin disc that is rotating about x- or y-axis, the moment of inertia is $I = m r_{uav}^2/4$. Thus, with the assumption that the center of the UAV is the pivot, the angular acceleration can be obtained by substituting these equations into Equation 14.

$$\alpha = \frac{2\sqrt{d_{12_x}^2 + d_{12_y}^2}\,\mathbf{1_3^T}\mathbf{R_{B_2I}}\mathbf{a_{dw_I}}(\mathbf{d_{12_z}})}{r_{uav}^2} \tag{17}$$

If the center of the downwash force is exerted near the x- or y-axis of the UAV body frame, then the torque can be considered into the pitch or roll angle directly. However, if the center of the downwash force is not exerted near the x- or y-axis, the UAV pitch and roll angles are affected simultaneously.

In Figure 3, with the assumption that the orientations of the two are the same and UAV2 is below UAV1, the circle presented in the dash line is the downwash air flow generated by UAV1. The d_{12_x} and d_{12_y} are the values from Equation 9, the green dot is the point where the center of the downwash force is exerted on, and $\beta = tan^{-1}(|d_{12_x}|/|d_{12_y}|)$ is the angle to refer where the green dot is.

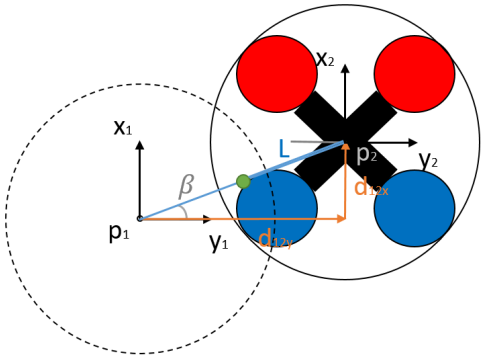

Fig. 3 Top view of the airflow region and the bottom UAV in the UAV1 body frame

The roll angular acceleration is positive if $d_{12_y} < 0$, negative otherwise. The pitch angular acceleration is positive if $d_{12_x} > 0$, negative otherwise. If the β angle is larger than 10° and smaller than 80°, it is assumed that the air flow hits a single rotor, therefore the UAV will row and pitch with equivalent amount. The angular acceleration due to the downwash effect can be concluded as follows,

$$\begin{cases} \ddot{\psi}_{torq} = \pm\alpha,\ \ddot{\theta}_{torq} = 0, & if\ \beta \leq 10^\circ \\ \ddot{\theta}_{torq} = \pm\alpha,\ \ddot{\psi}_{torq} = 0, & if\ \beta \geq 80^\circ \\ \ddot{\psi}_{torq} = \pm\sqrt{2}\alpha,\ \ddot{\theta}_{torq} = \pm\sqrt{2}\alpha, & if\ 10^\circ < \beta < 80^\circ \end{cases} \tag{18}$$

III. Path Planning Algorithms

Path planning algorithms allow a group of UAVs to travel from their initial locations to the final locations without collision. In this paper, the path planning problem assumes the following scenarios:

- There are n number of UAVs flying in the three-dimensional environment.
- Each UAV has a unique initial position and a unique final location.
- Each UAV is restricted by a maximum allowance velocity.
- There is no obstacles in the environment so only inter-UAV collisions shall be aware of.

A. Flocking Algorithm

This section introduces the flocking algorithm, which is an algorithm inspired by the collective behaviour of a group of birds. The group of birds has one shared target. They fly close to each other but collisions rarely happen between them. The flocking behaviour is first simulated by Reynolds [15] and he proposed three rules: collision avoidance, velocity matching, and flock centering. These rules represent that an individual shall avoid crowding neighbors, move at the average speed of neighbors, and direct in the average heading of neighbors. Olfati-Saber [16] proposed a set of mathematics background and theoretical framework for the flocking algorithm based on Reynolds' three rules. Each agent/bird is controlled by three force-based terms: navigational feedback, gradient-based term, and velocity-consensus term. The navigational feedback leads the agent toward the target. The gradient-based term consists of both attractive and repulsive force and tried to keep all agents' relative distances close to a chosen distance. The velocity-consensus term tries to keep all agents having the same speed.

Semnani et al. [12] modified Olfati-Saber's mathematical work to one that is applicable to path planning for multi-UAV where each UAV has a unique target. They eliminated the velocity-consensus term since the UAVs do not need to match velocities. They modified the gradient-based term to consist of the repulsive force only since each UAV has its own destination and still needs to avoid colliding with each other. The navigational feedback is unmodified. The UAV dynamics and the mathematics expression for the force ($\mathbf{f}$) acting on a single UAV i are as follows,

$$\begin{cases} \dot{\mathbf{p}}_\mathbf{i} = \mathbf{v}_\mathbf{i} \\ \dot{\mathbf{v}}_\mathbf{i} = \mathbf{f}_\mathbf{i} \end{cases} \tag{19}$$

$$\mathbf{f}_\mathbf{i} = \begin{cases} \mathbf{0}, & if\ \mathbf{v_i}^T \bar{\mathbf{f}}_\mathbf{i} > 0\ and\ ||\mathbf{v_i}|| \geq V_{max} \\ \bar{\mathbf{f}}_\mathbf{i} = \mathbf{f}_\mathbf{i}^\mathbf{R} + \mathbf{f}_\mathbf{i}^\gamma, & otherwise \end{cases} \tag{20}$$

$$\mathbf{f}_\mathbf{i}^\mathbf{R} = \sum_{j \in N_i} \left(\phi(||\mathbf{p_j} - \mathbf{p_i}||) \frac{\mathbf{p_j} - \mathbf{p_i}}{||\mathbf{p_j} - \mathbf{p_i}||} \right) \tag{21}$$

$$\phi(z) = \begin{cases} -\rho(z - r_\alpha)^2, & 0 < z < r_\alpha \\ 0, & z \geq r_\alpha \end{cases} \tag{22}$$

$$\mathbf{f}_\mathbf{i}^\gamma = -c_i(\mathbf{p_i} - \mathcal{T}_\mathbf{i}) - c_2(\mathbf{v_i}) \tag{23}$$

where $\mathbf{p}, \mathbf{v}, \mathbf{f}_\mathbf{i}^\mathbf{R}, \mathbf{f}_\mathbf{i}^\gamma \in \mathbb{R}^3$ are the position, velocity, repulsive force, and navigational feedback, respectively. V_{max} is the maximum allowable velocity, N_i is the set of neighbors of UAV i, ρ is a positive repulsive gradient that is used to make sure the repulsive force is high enough to repel UAVs from getting too close, r_α is the interaction radius, c_1, c_2 are positive constants, and $\mathcal{T}$ is the set of target positions. On one hand, an UAV will only be controlled by the navigational feedback and move toward its target if there is no neighboring UAV within its interaction area. The interaction area defined in Equation 22 is a sphere with a radius of r_α to allow the UAVs to avoid collisions from all three directions equally important. On the other hand, when there is one or more UAVs inside its interaction area, the repulsive force will contribute and dominate in controlling an UAV since the repulsive gradient (ρ) is set large. The smaller the ρ value, the higher the encountering probability. The closer the two UAVs, the higher the repulsive force.

When UAVs are modelled as cylinders, two UAVs are considered within each other's interaction region when their horizontal distance difference is within the interaction radius r_α and their attitude difference is within half of the interaction height h_α. The flocking algorithm repulsive force of the host UAV i (f_i^R) presented in [12] and Equations 21 and 22 is modified to account for the cylindrical height h_α by adding an altitude difference constraint.

$$\mathbf{f}_\mathbf{i}^\mathbf{R} = \sum_{j \in N_i} \phi(\mathbf{p_j} - \mathbf{p_i}) \tag{24}$$

$$\phi(\mathbf{\Delta p}) = \begin{cases} \begin{bmatrix} -\rho \left(\sqrt{\Delta p_x^2 + \Delta p_y^2} - r_\alpha \right)^2 \frac{\Delta p_x}{||\mathbf{\Delta p}||} \\ -\rho \left(\sqrt{\Delta p_x^2 + \Delta p_y^2} - r_\alpha \right)^2 \frac{\Delta p_y}{||\mathbf{\Delta p}||} \\ -\rho \left(|\Delta p_z| - h_\alpha/2 \right)^2 \frac{\Delta p_z}{||\mathbf{\Delta p}||} \end{bmatrix}, & if\ 0 < \sqrt{\Delta p_x^2 + \Delta p_y^2} < r_\alpha\ and\ |\Delta p_z| < h_\alpha/2 \\ [0,\ 0,\ 0]^T, & otherwise \end{cases} \tag{25}$$

where Δp_x is the x-component of $\mathbf{\Delta p}$, and similarly for Δp_y and Δp_z. The interaction height in Equation 25 is divided to half because the distance to consider starts from the center of the UAV, such as the radius is used instead of diameter when considering for the x- and y-directions. The repulsive force calculated by Equation 25 will kick in when the host UAV i sense any of its neighbors is within its cylindrical interaction area with the radius of r_α and the height of h_α.

B. Optimal Reciprocal Collision Avoidance (ORCA) Algorithm

The ORCA algorithm is a velocity-based algorithm presented by van den Berg [13]. This algorithm is designed for the multi-UAV navigation problem. It is the first algorithm that can guarantee local collision-free motion for a large number of UAVs in a dense environment.

In the ORCA algorithm, each UAV takes action based on assuming the other UAVs make similar behavior reasoning. Each UAV knows the other UAVs' information such as position, velocity, and radius. An UAV utilizes the other UAVs'

information to predict over a time horizon (τ) and obtain a set of velocities that would cause inter-UAV collision before τ time if selected. Therefore, with this velocity constraint, the algorithm optimizes the performance by calculating the ORCA half-plane based on the optimal/current velocity of the UAV. When the UAVs are considered as cylinders, the cylindrical height h_α is also used to determine the ORCA half-plane.

An UAV would obtain an ORCA half-plane for each of the other UAVs. The intersection of all the ORCA half-planes ($ORCA^\tau$) is the set of velocities where the UAV can choose from and guarantee collision-free for τ time. The new velocity would be the velocity from $ORCA^\tau$, which is closest to the preferred velocity, where the preferred velocity is the velocity that leads the UAV toward its goal.

$$v^{new} = \underset{v \in ORCA^\tau}{\operatorname{argmin}} ||v - v^{pref}|| \tag{26}$$

C. Summary

For both algorithms, every UAV does not need to communicate with each other and have perfect sensing. This means that an UAV is able to infer the exact shape, position, and velocity of obstacles and other UAVs in the environment. They are designed to solve multi-UAV motion planning problems and guarantee collision-free in dense environments.

On one hand, a flocking algorithm is a force-based approach where the goal induces an attractive force and nearby UAVs induce the repulsive force. The resultant force is not limited, so the UAV's velocity commanded may change from maximum allowable velocity V_{max} to minimum allowable velocity $-V_{max}$ in a single time step. On the other hand, the ORCA algorithm is a velocity-based algorithm and guarantees collision-free for τ time. To prevent the velocity jump caused by the flocking algorithm, an acceleration limiter a_{max} is used on the resultant force of navigational feedback and repulsive force.

IV. Simulation results

A. Downwash Model

The worst downwash effect happens when the bottom UAV is hovering and the top UAV fly from above it. This case maximizes the time and surface are the bottom UAV suffers from the downwash air flow. Therefore, to test for the downwash model, the top UAV is flying from (0, 1, 1.8) to (2, 1, 1.8) and the bottom UAV is hovering at (1, 1, 1.5). A simple UAV dynamics from [17] is adapted, and the maximum allowable roll and pitch angles are $0.3\,rad$. The navigational feedback of the flocking algorithm is used for UAVs to move to their desired positions. The parameters used are: time step $\Delta t = 0.01\,s$, and maximum allowable velocity $V_{max} = 1.5\,m/s$, and the parameters for navigation feedback $c_1 = 7$ and $c_2 = 9$. Figure 4 shows the bottom UAV's position when it suffers from three different downwash cases. The first case is the tilted downwash effect is not considered (Figure 4a), the second case is when the downwash torque is not considered (Figure 4b), and the third case is when the whole downwash model is considered (Figure 4c). In the first case, the bottom UAV only suffers from the downward force and is pushed down for 1.29 m. In the second case, the bottom UAV travels downward for 0.97 m and horizontally for 1.12 m due to the tilted downwash air flow. The vertical distance travelled by the UAV in this case is less than the first case because the horizontal movement lets the UAV suffer less from the vertical downwash force. In the third case, the bottom UAV travels downward for 0.91 m and horizontally for 1.06 m. The horizontal movement of the UAV is less than the one is the second case because the downwash torque acts counter to the tilted downwash force. For the top UAV to go from its initial position to its desired position, it takes 2.88 s. It takes 3.56 s, 3.35 s, 3.29 s, to complete the first, the second, and the third case, respectively.

B. Path Planning Algorithms with Effective Downwash Effect

The proposed downwash force model is simulated to observe the severity of how the downwash force can influence an UAV and how the cylindrical UAV model can benefit the path planning algorithms. Both the flocking algorithm and the optimal reciprocal collision avoidance (ORCA) algorithm have been successfully coded, executed, and simulated in 2D and 3D environments. The research team that proposed the ORCA algorithm provides the open-source code online [18]. Modification is made on [18] to account for cylindrical UAV model.

To compare for the performance of the flocking and ORCA algorithms, the parameters in the algorithms that have the same functionality are set to the same values. The parameters are: interaction radius r_α, interaction height h_α, radius of an UAV $r_{uav} = 0.15\,m$, time step $\Delta t = 0.01\,s$, and maximum allowable velocity $V_{max} = 1.5\,m/s$. The parameters used

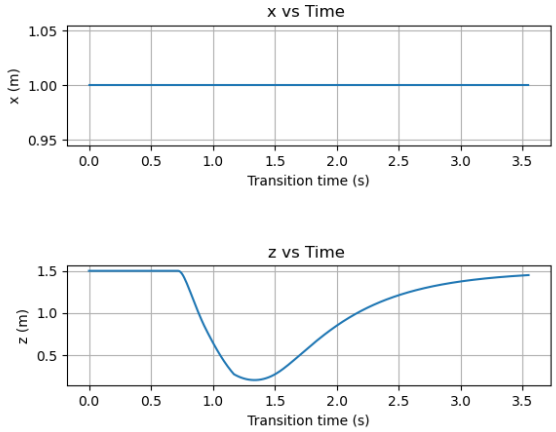

(a) Bottom UAV's positions without tilted downwash effect

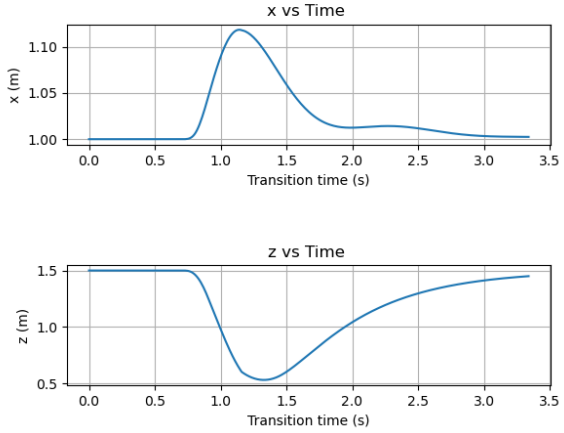

(b) Bottom UAV's position with downwash force

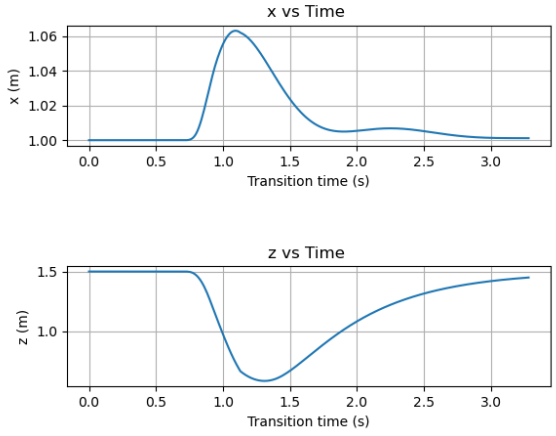

(c) Bottom UAV's position with downwash force and torque

Fig. 4 Bottom UAV's position

for the flocking algorithm only are: maximum allowable acceleration $a_{max} = 5.0\,m/s^2$, repulsive gradient $\rho = 1000$, and the parameters for navigation feedback $c_1 = 7$ and $c_2 = 9$. The time horizon τ used for the ORCA algorithm is set

	Flocking Algorithm			
	Spherical		Cylindrical	
r_α (m)	0.45	0.50	0.45	0.50
$h_\alpha/2$ (m)	N/A	N/A	0.60	0.60
Transition Time (s)	6.98	7.12	7.93	8.34
Success Rate (%)	44	69	59	71
	ORCA Algorithm			
	Spherical		Cylindrical	
r_α (m)	0.45	0.50	0.45	0.50
$h_\alpha/2$ (m)	N/A	N/A	0.60	0.60
Transition Time (s)	6.93	5.98	6.34	6.84
Success Rate (%)	32	37	36	41

Table 1 Simulation results of the path planning algorithms with different models

to be r_α/V_{max}.

To compare for the performance of the spherical and the cylindrical UAV models under a 3D dense environment with downwash effect, the simulation environment setup is having 10 UAVs hovering inside a space with a width of 2 meters, length of 2 meters, and height of 1 meter, and 10 UAVs travel from one side of this space to another side.

The initial and target positions of these 20 UAVs are randomly generated. Table 1 shows the transition time performance and the success rate averaged over 100 outcomes for spherical and cylindrical UAV models for the flocking and ORCA algorithms. The transition time is the total time for all UAVs to travel from initial to target positions, and the higher this value, the worse the performance and the less efficient the UAV model. The success rate is the number of times that UAVs successfully arrive at the targets without getting collided or stuck, and the higher this value, the better.

As shown in Table 1, when the spherical and cylindrical models have the same radius, the performance of the cylindrical model has a higher success rate. This conclusion is supported by both the flocking and the ORCA algorithms, and can prove that the cylindrical model prevents the UAVs from a collision due to the downwash effect. The ORCA algorithm has a lower success rate compared to the flocking algorithm because it takes its current velocity into account while calculating for the next velocity and changes velocity gradually. An UAV would not be able to avoid nearby UAV fast enough. For the results of the flocking algorithm, it verifies that the larger the interaction area, the worse the transition time. However, this is not the case for the ORCA algorithm because the time horizon changes as the interaction area changes and the time for the algorithm to plan for the UAV movement also changes.

V. Conclusion

In this paper, a downwash model that can predict the downwash force on an UAV without aid from any instrument is developed. The downwash model includes the determination of the magnitude and the direction of the downwash effect. The pose and the position of an UAV that counters the downwash air flow can be predicted. Simulates demonstrates how an UAV can be influenced by the downwash effect. A flocking algorithm and an optimal reciprocal collision avoidance (ORCA) algorithm are modified to consider the cylindrical UAV model. Simulations verified that the cylindrical model improves the path planning success rate in a 3D dense environment with effective downwash force.

Future considerations include the downwash model and the cylindrical UAV model improvements. Many assumptions are made during the downwash model development, so many elements are not considered. For example, the influence of the propellers when the downwash air flow hits, the downwash air flow delay, the spread-out air flow velocity, and the air flow velocity merges from all four rotors. These are some of the elements that can be considered to improve the downwash model. Simulation results show that the larger the interaction area, the worse the time performance. Therefore, a method that can balance the safety and performance can be developed.

Acknowledgments

Sponsorship information and funding data are included here.

References

[1] Scherer, J., and Rinner, B., "Persistent multi-UAV surveillance with energy and communication constraints," *2016 IEEE International Conference on Automation Science and Engineering (CASE)*, IEEE, 2016, pp. 1225–1230.

[2] Chen, Y., Yu, J., Su, X., and Luo, G., "Path planning for multi-UAV formation," *Journal of Intelligent & Robotic Systems*, Vol. 77, No. 1, 2015, pp. 229–246.

[3] Ang, K. Z., Dong, X., Liu, W., Qin, G., Lai, S., Wang, K., Wei, D., Zhang, S., Phang, S. K., Chen, X., et al., "High-precision multi-UAV teaming for the first outdoor night show in Singapore," *Unmanned Systems*, Vol. 6, No. 01, 2018, pp. 39–65.

[4] Kothari, M., Postlethwaite, I., and Gu, D.-W., "Multi-UAV path planning in obstacle rich environments using rapidly-exploring random trees," *Proceedings of the 48h IEEE Conference on Decision and Control (CDC) held jointly with 2009 28th Chinese Control Conference*, IEEE, 2009, pp. 3069–3074.

[5] Shao, S., Peng, Y., He, C., and Du, Y., "Efficient path planning for UAV formation via comprehensively improved particle swarm optimization," *ISA transactions*, Vol. 97, 2020, pp. 415–430.

[6] Binol, H., Bulut, E., Akkaya, K., and Guvenc, I., "Time optimal multi-uav path planning for gathering its data from roadside units," *2018 IEEE 88th Vehicular Technology Conference (VTC-Fall)*, IEEE, 2018, pp. 1–5.

[7] Yeo, D., Sydney, N., Paley, D. A., and Sofge, D., "Onboard flow sensing for downwash detection and avoidance with a small quadrotor helicopter," *AIAA Guidance, Navigation, and Control Conference*, 2015, pp. 1–10.

[8] Wu, Y., Qi, L., Zhang, H., Musiu, E. M., Yang, Z., and Wang, P., "Design of UAV downwash airflow field detection system based on strain effect principle," *Sensors*, Vol. 19, No. 11, 2019, p. 2630.

[9] Preiss, J. A., Hönig, W., Ayanian, N., and Sukhatme, G. S., "Downwash-aware trajectory planning for large quadrotor teams," *2017 IEEE/RSJ International Conference on Intelligent Robots and Systems (IROS)*, IEEE, 2017, pp. 250–257.

[10] Hönig, W., Preiss, J. A., Kumar, T. S., Sukhatme, G. S., and Ayanian, N., "Trajectory planning for quadrotor swarms," *IEEE Transactions on Robotics*, Vol. 34, No. 4, 2018, pp. 856–869.

[11] Ferrera, E., Alcántara, A., Capitán, J., Castaño, A. R., Marrón, P. J., and Ollero, A., "Decentralized 3D Collision Avoidance for Multiple UAVs in Outdoor Environments," *Sensors*, 2018.

[12] Semnani, S. H., de Ruiter, A. H., and Liu, H. H., "Force-Based Algorithm for Motion Planning of Large Agent," *IEEE Transactions on Cybernetics*, 2020.

[13] Van Den Berg, J., Guy, S. J., Lin, M., and Manocha, D., "Reciprocal n-body collision avoidance," *Robotics Research*, Springer, 2011, pp. 3–19.

[14] Cushman-Roisin, B., *Environmental Fluid Mechanics*, John Wiley & Sons, Inc., 2019.

[15] Reynolds, C. W., "Flocks, Herds, and Schools: A Distributed Behavioral Model," *Computer Graphics*, Vol. 21, No. 4, 1987, pp. 25–34.

[16] Olfati-Saber, R., "Flocking for Multi-Agent Dynamic Systems: Algorithms and Theory," *IEEE Trans. Automatic Control*, Vol. 51, No. 3, 2006, pp. 401–420.

[17] Liao, J., Liu, C., and Liu, H. H. T., "Model Predictive Control for Cooperative Hunting in Obstacle Rich and Dynamic Environments," *IEEE International Conference on Robotics and Automation*, Montreal, Canada, 2021, pp. 1–8.

[18] *ROV2 Library: Optimal Reciprocal Collision Avoidance in Three Dimensions*, https://github.com/snape/RVO2-3D, 2021.